

Correlation Effects in Electrically Tunable Platforms in Low-dimensional Electron Systems

徐晨軒

Chen-Hsuan Hsu

Institute of Physics, Academia Sinica, Taiwan

2025 IOP Mini workshop

June 25th, 2025

 [CHH et al., Phys. Rev. B 108, L121409 \(2023\)](#); [Wang and CHH, 2D Mater. 11, 035007 \(2024\)](#);
[CHH, Nanoscale Horiz. 9, 1725 \(2024\)](#); [Chang, Saito, and CHH, arXiv:2412.14065](#)

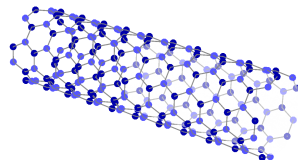
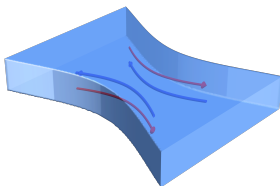
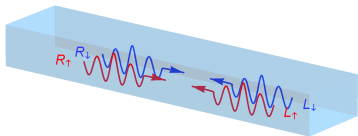
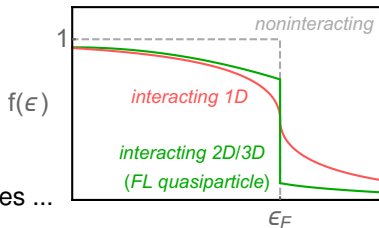
 Hao-Chien Wang (IoP, AS → UIUC), Kazuma Saito (Tokyo Unvi Sci. & IoP, AS), Yung-Yeh Chang (IoP, AS), Hsin Lin (IoP, AS), Yi-Chun Hung & Arun Bansil (Northeastern), Jelena Klinovaja & Daniel Loss (Basel)

 National Science and Technology Council (NSTC), Institute of Physics & Academia Sinica, Taiwan

Peculiar properties of interacting electrons in 1D

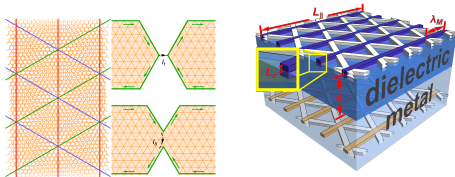
- Correlation effects in any interacting 1D systems
- Power-law suppression of density of states $\rho(\epsilon_F) \rightarrow 0$
 \Rightarrow power-law behavior of correlation functions
- Tomonaga-Luttinger liquid (TLL):
 - correlation effects with observable features
 - platforms: nanowires, quantum point contact, nanotubes ...

occupation number at $T = 0$



Correlated electrons in low-dimensional nanoscale systems

- Recent interest: Generalizations of Tomonaga-Luttinger liquids (TLL) to other platforms
- Beyond 1D:
domain wall network appearing in
twisted bilayer graphene (TBG)
⇒ coupled network of TLL
- Beyond spin-degenerate systems:
spin-momentum-locked boundary states
⇒ helical liquids



(Fractional) quantum anomalous Hall effect in TBG

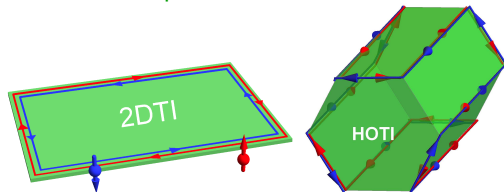
[CHH et al., Phys. Rev. B 108, L121409 \(2023\)](#)

Superconductivity in TBG network

[Wang and CHH, 2D Mater. 11, 035007 \(2024\)](#)

2D helix in TBG network

[Chang, Saito, and CHH, arXiv:2412.14065](#)



Topological superconductivity in double helical liquids

[CHH, Nanoscale Horiz. 9, 1725 \(2024\)](#)

Time-reversal soliton corner modes in HOTI

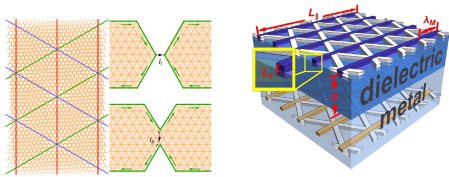
[Hung, Wang, CHH et al., PRB 110, 035125 \(2024\)](#)

Majorana zero modes in high spin Chern insulators

[Hung, CHH, and Bansil, PRB 111, 245145 \(2025\)](#)

Correlated electrons in low-dimensional nanoscale systems

- Generalizations of Tomonaga-Luttinger liquids (TLL) to other platforms
- Beyond 1D:
domain wall network appearing in
twisted bilayer graphene (TBG)
⇒ coupled network of TLL
- Beyond spin-degenerate systems:
spin-momentum-locked boundary states
⇒ helical liquids



(Fractional) quantum anomalous Hall effect in TBG

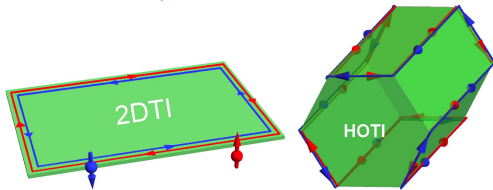
[CHH et al., Phys. Rev. B 108, L121409 \(2023\)](#)

Superconductivity in TBG network

[Wang and CHH, 2D Mater. 11, 035007 \(2024\)](#)

2D helix in TBG network

[Chang, Saito, and CHH, arXiv:2412.14065](#)



Topological superconductivity in double helical liquids
[CHH, Nanoscale Horiz. 9, 1725 \(2024\)](#)

Time-reversal soliton corner modes in HOTI

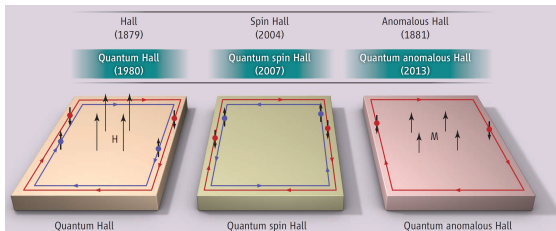
[Hung, Wang, CHH et al., PRB 110, 035125 \(2024\)](#)

Majorana zero modes in high spin Chern insulators

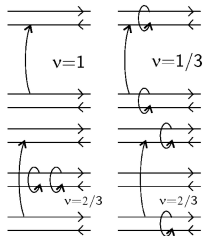
[Hung, CHH, and Bansil, PRB 111, 245145 \(2025\)](#)

Trio of quantum Hall-related phenomena

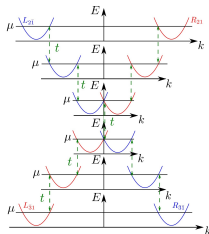
- coupled-wire or network construction



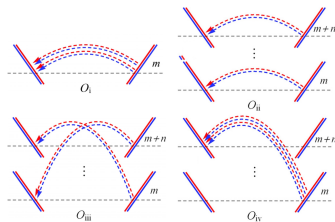
Oh, Science 2013



Kane et al., PRL 2002;



Klinovaja and Tserkovnyak, PRB 2014;



CHH et al., Phys. Rev. B 108, L121409 (2023)

Outline

Electrically tunable correlated domain wall network in moiré structures

Tunable platform for topological superconductivity and zero modes

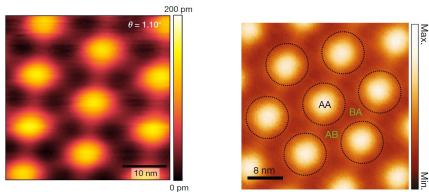
Outline

Electrically tunable correlated domain wall network in moiré structures

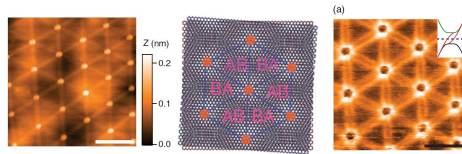
Tunable platform for topological superconductivity and zero modes

2D network of 1D domain wall channels in twisted nanostructures

- STM images of domain walls between AB- and BA-stacking areas

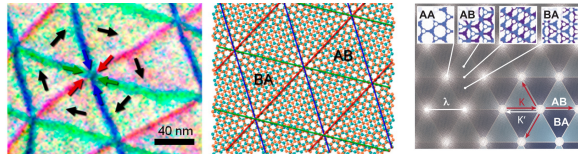


Kerelsky et al., Nature 2019; Jiang et al., Nature 2019

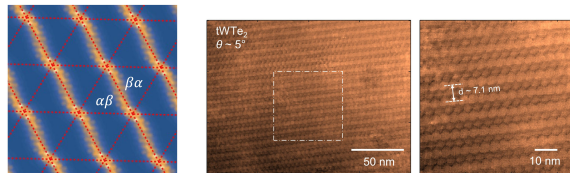


Huang al., PRL 2018

- TEM and transport features of domain walls



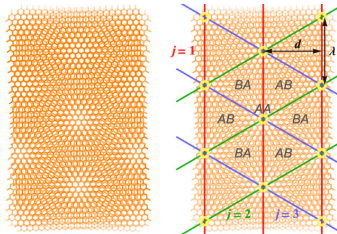
Alden et al., PNAS 2013; Rickhaus et al., Nano Lett. 2018
1D channels in chiral twisted trilayer graphene and twisted bilayer WTe_2



Nakatsuji et al., PRX 2023; Wang et al., Nature 2022

2D network formed by domain wall modes of moiré bilayer systems

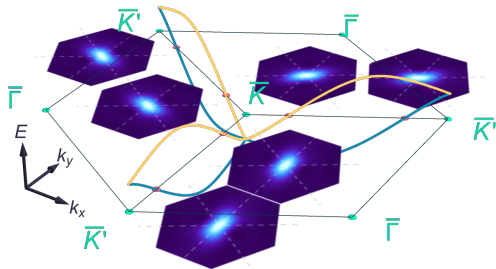
- In the presence of an interlayer bias:
local spectral gap with opposite signs in the AB- and BA-stacking regions
⇒ a mesoscopic network of domain walls



- (Quasi-)1D interacting electron systems: Tomonaga-Luttinger liquid (TLL)
- Domain walls in TBG: triangular network of coupled Tomonaga-Luttinger liquids
- **Correlation** effects and $e-e$ interactions in the network of moiré structures:
 - no formation of flat bands
 - not limited to the “magic angle”

Charge density distribution of the low-energy states

- Continuum model of twisted bilayer graphene (TBG) (+ interlayer bias here)
Bistritzer & MacDonald, PNAS 2011; Nam & Koshino, PRB 2017; Tarnopolsky et al. PRL 2019
- Spatial profile of the charge density ρ_{2D} for low-energy states:
following the triangular domain wall network



- 2D global fitting of the charge density distribution

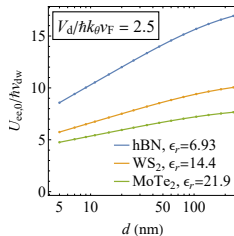
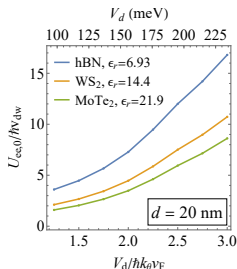
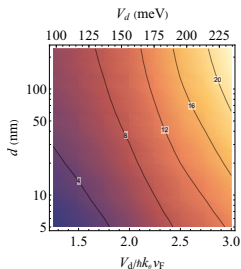
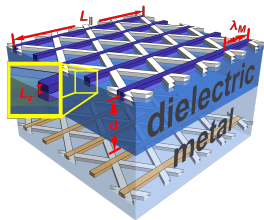
$$\rho_{2D}(\vec{r}) = C_0 \sum_{j=0}^2 \sum_m \sum_{\delta} \rho_{\delta,m}^{\text{dw}} (\mathcal{R}_{2j\pi/3} \vec{r})$$

- ρ_{2D} depending on interlayer bias V_d and hybridization α_{AB}
 \Rightarrow offering **tunability**
 - $V_d / \hbar v_F k_{\theta} = 1.5$
 - $\alpha_{AB} = 1.4$ ($\theta = 0.5^{\circ}$)

- blue/yellow curves: energy bands intersecting at μ along $\bar{K}-\bar{K}'$ lines within mBZ

$e-e$ interaction strength in 2D triangular domain wall network

- TBG stacked with a dielectric layer of thickness d and a metallic gate
 $\Rightarrow d$ as a screening length



- Screened Coulomb interaction strength within a domain wall (“intrawire” interaction)

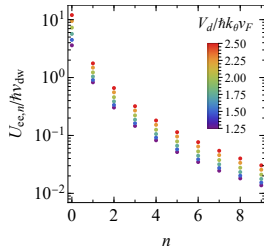
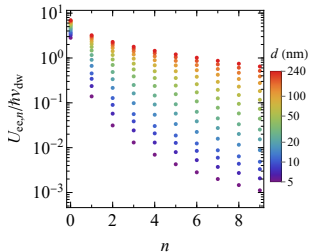
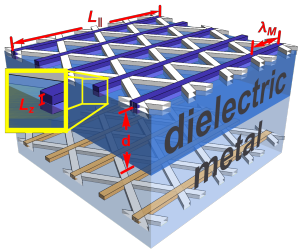
$$U_{ee,0} = \frac{e^2 L_y}{4\pi\epsilon_0} \int d^3 \mathbf{x} \int d^3 \mathbf{x}' \left[\frac{\rho_m^{\text{dw}}(\mathbf{x}) \rho_m^{\text{dw}}(\mathbf{x}')}{|\mathbf{x} - \mathbf{x}'|} + \frac{\rho_m^{\text{dw}}(\mathbf{x}) \rho_m^{\text{image}}(\mathbf{x}')}{|\mathbf{x} - \mathbf{x}'|} \right]$$

- Electrically tunable through *in-situ* bias, screening length, and dielectric material
 \Rightarrow enhanced by ~ 7 fold

Interaction strength between parallel domain walls

- Interaction strength between n th-nearest-neighbor domain walls (“interwire” interaction)

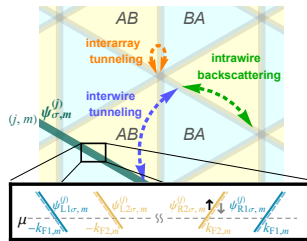
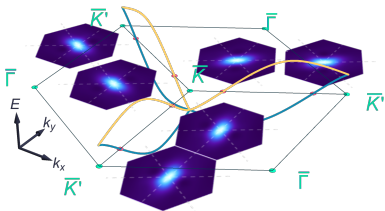
$$U_{ee,n} = \frac{e^2 L_y}{4\pi\epsilon_0} \int d^3\mathbf{x} \int d^3\mathbf{x}' \left[\frac{\rho_m^{\text{dw}}(x)\rho_{m+n}^{\text{dw}}(x')}{|\mathbf{x} - \mathbf{x}'|} + \frac{\rho_m^{\text{dw}}(x)\rho_{m+n}^{\text{image}}(x')}{|\mathbf{x} - \mathbf{x}'|} \right]$$



- varying dielectric layer thickness, with $V_d/\hbar v_F k_{\theta} = 1.5$
- varying interlayer bias, with $d = 20$ nm
- Electrically tunable interaction strength in the domain wall network

Bosonization

- Low-energy regime: linear dispersion near the Fermi level



- Fermion field $\psi_{\ell\delta\sigma,m}^{(j)}$ for electrons in the m th domain wall of the j th array

$$\psi_{\ell\delta\sigma,m}^{(j)}(x) = \frac{U_{\ell\delta\sigma,m}^j}{\sqrt{2\pi a}} e^{i\ell k_{F\delta,m}^{(j)} x} e^{\frac{i}{2} \left[-\ell(\phi_{cs,m}^j + \delta\phi_{ca,m}^j) - \ell\sigma(\phi_{ss,m}^j + \delta\phi_{sa,m}^j) + (\theta_{cs,m}^j + \delta\theta_{ca,m}^j) + \sigma(\theta_{ss,m}^j + \delta\theta_{sa,m}^j) \right]}$$

- Subscripts for fermion species (8 gapless modes per domain wall):
 - $\ell = R$ ($\ell = L$): right-moving (left-moving) mode
 - $\delta = 1$ ($\delta = 2$): outer (inner) branch of the energy bands
 - $\sigma = \uparrow$ ($\sigma = \downarrow$): spin-up (spin-down) state
- Illustrations of various microscopic processes in the domain wall network

Bosonized model for the correlated domain wall network

- Bosonized operators:
 - charge density $\propto \partial_x \phi_{cP,m}^j$
 - charge current $\propto \partial_x \theta_{cP,m}^j$

- Hamiltonian in the bosonized form:

$$H_{ee} = \sum_{j=0}^2 \sum_{\nu \in \{c,s\}} \sum_{P \in \{s,a\}} H_{\nu P}^{(j)}$$

$$H_{cP}^{(j)} = \sum_m \sum_n \int \frac{dx}{2\pi} \left[U_{\phi_{cP,n}}^{(j)} \left(\partial_x \phi_{cP,m}^j \right) \left(\partial_x \phi_{cP,m+n}^j \right) + U_{\theta_{cP,n}}^{(j)} \left(\partial_x \theta_{cP,m}^j \right) \left(\partial_x \theta_{cP,m+n}^j \right) \right]$$

$$H_{sP}^{(j)} = \sum_m \int \frac{\hbar dx}{2\pi} \left[\frac{u_{sP}}{K_{sP}} \left(\partial_x \phi_{sP,m}^j \right)^2 + u_{sP} K_{sP} \left(\partial_x \theta_{sP,m}^j \right)^2 \right]$$

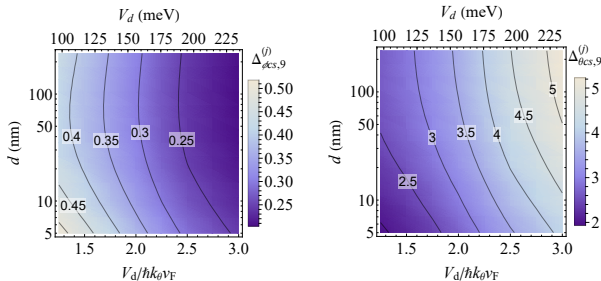
- $\nu \in \{c, s\}$ for charge/spin sector (symmetric/antisymmetric combination of $\sigma = \uparrow, \downarrow$)
- $P \in \{s, a\}$ for symmetric/antisymmetric combination of $\delta = 1, 2$
- Coulomb (density-density) interaction
 - \Rightarrow forward-scattering terms ($R \leftrightarrow R$ & $L \leftrightarrow L$) in the quadratic form $\propto \partial_x \phi_{cP,m}^j \partial_x \phi_{cP,m+n}^j$
 - \Rightarrow **diagonalizable**

Correlation effects from electron-electron interactions

- Interaction-dependent parameters related to scaling exponents of correlation functions:

$$\left\langle e^{-\sqrt{2}i\phi_{cs,m}^{(j)}(\vec{x})} e^{\sqrt{2}i\phi_{cs,m}^{(j)}(0)} \right\rangle_{ee} \propto \left| \frac{a}{\vec{x}} \right|^{\Delta_{\phi_{cs,m}}^{(j)}}, \quad \left\langle e^{-\sqrt{2}i\theta_{cs,m}^{(j)}(\vec{x})} e^{\sqrt{2}i\theta_{cs,m}^{(j)}(0)} \right\rangle_{ee} \propto \left| \frac{a}{\vec{x}} \right|^{\Delta_{\theta_{cs,m}}^{(j)}}$$

- scaling parameters $\Delta \rightarrow 1$ for noninteracting electrons
- larger deviation from the unity due to the stronger correlation
- Electrically tunable exponents through the interlayer bias V_d and screening length d :

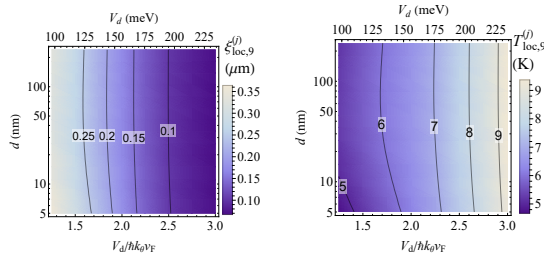


Localization induced by potential disorder

- Effective action from disorder-induced backscattering process:

$$\frac{S_{\text{dis},m}^{(j)}}{\hbar} = -\frac{\tilde{D}_{\text{b},m}^{(j)} v_{\text{dw}}^2}{2\pi a^3} \sum_{rr'\delta} \int d\tau d\tau' dx \cos \left[\phi_{cs,m}^{j,r}(x, \tau) + \delta\phi_{ca,m}^{j,r}(x, \tau) - \phi_{cs,m}^{j,r'}(x, \tau') - \delta\phi_{ca,m}^{j,r'}(x, \tau') \right] \\ \times \cos \left[\phi_{ss,m}^{j,r}(x, \tau) + \delta\phi_{sa,m}^{j,r}(x, \tau) \right] \cos \left[\phi_{ss,m}^{j,r'}(x, \tau') + \delta\phi_{sa,m}^{j,r'}(x, \tau') \right]$$

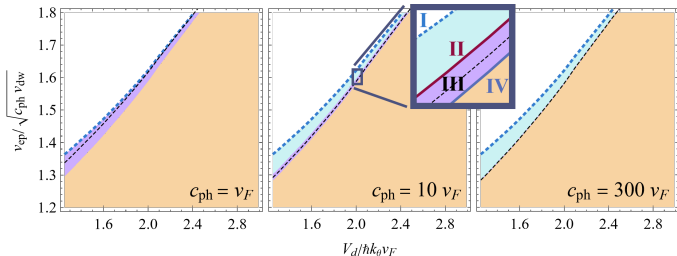
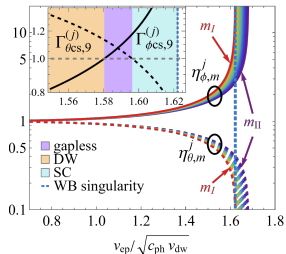
- Localization for a sufficiently large sample ($L > \xi_{\text{loc}}$) at sufficiently low temperatures ($T < T_{\text{loc}}$)



Wang and [CHH](#), 2D Mater. 11, 035007 (2024)

- more pronounced as one attempts to scale up devices
- localization length and temperature also **electrically tunable** within a sample

Electrically tunable correlated domain wall network



Wang and [CHH](#), 2D Mater. 11, 035007 (2024)

- Various phases: correlated domain wall network, density wave, superconductivity, e-phonon-coupled liquid
- Distinct behavior upon varying phonon velocity:
 - low-velocity regime: no pairing instability
 - intermediate regime: **pairing instability** for sufficiently large electron-phonon coupling
- Electrically tunable phase transitions

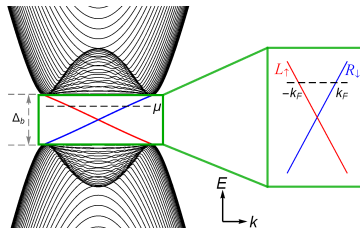
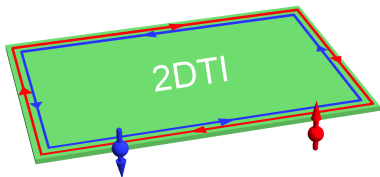
Outline

Electrically tunable correlated domain wall network in moiré structures

Tunable platform for topological superconductivity and zero modes

Helical edge channels in two-dimensional topological insulator (2DTI)

- Gapped 2D bulk and gapless 1D edges
- Topologically protected *helical edge channels* in time-reversal-invariant materials: electrons with opposite spins flow in the opposite directions

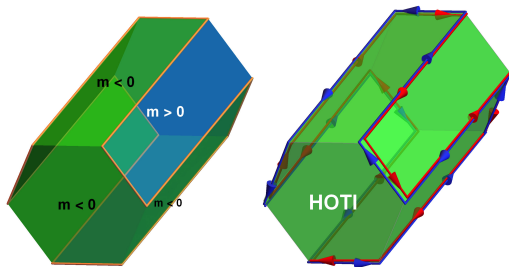


- Predictions and experimental realizations:
 - HgTe quantum wells Bernevig et al., Science 2006; Konig et al., Science 2007
 - InAs/GaSb heterostructures Liu et al., PRL 2008; Knez et al., PRL 2011
 - monolayer $1T'$ -WTe₂ Tang et al., Nat. Phys. 2017
 - bismuthene on SiC Reis et al., Science 2017
 - twisted bilayer MoTe₂ Kang et al., Nature 2024

⋮

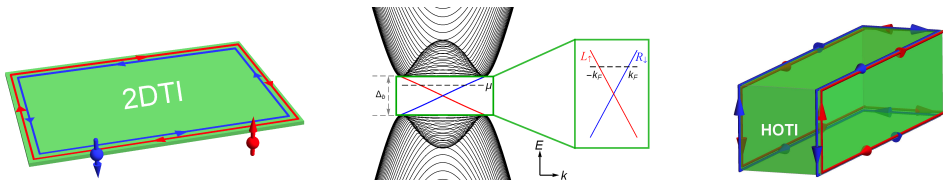
Helical hinge channels in higher-order topological insulators (HOTI)

- Gapped bulk and surfaces in 3D 2nd-order topological insulator
- Surface gap changes its sign with the surface orientation
⇒ surface-dependent Dirac mass: $m(\hat{n})$
⇒ gapless states at the hinges between two surfaces with the opposite signs



- Candidate materials:
 - Bi (theory/exp: Schindler et al., Nat. Phys. 2018; Murani et al., PRL 2019; Jäck et al., Science 2019)
 - Bi_4Br_4 (theory/exp: Noguchi et al., Nat. Mater. 2021)
 - multilayer WTe_2 in T_d structure (theory/exp: Choi et al., Nat. Mater. 2021)
 - SnTe, Bi_2TeI , BiSe, BiTe (theory: Schindler et al., Sci. Adv. 2018)

Helical liquids formed by interacting electrons in helical channels



- Electrons in 2DTI edges or HOTI hinges: $H_{hl} = H_{kin} + H_{ee}$

- Kinetic energy:

$$H_{kin} = -i\hbar v_F \int dr \left(R_{\downarrow}^{\dagger} \partial_r R_{\downarrow} - L_{\uparrow}^{\dagger} \partial_r L_{\uparrow} \right)$$

- $e-e$ interaction (g_2, g_4 : interaction strength):

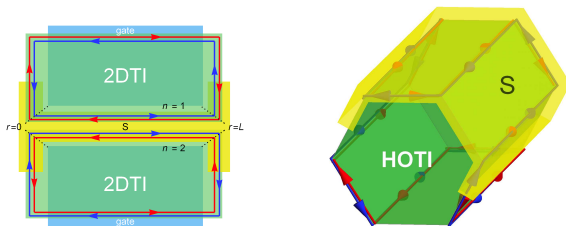
$$H_{ee} = g_2 \int dr R_{\downarrow}^{\dagger} R_{\downarrow} L_{\uparrow}^{\dagger} L_{\uparrow} + \frac{g_4}{2} \int dr \left[\left(R_{\downarrow}^{\dagger} R_{\downarrow} \right)^2 + \left(L_{\uparrow}^{\dagger} L_{\uparrow} \right)^2 \right]$$

- Spin-momentum locking nature + correlation effects in 1D confinement
 \Rightarrow **helical liquids**

Review article: [CHH et al., Semicond. Sci. Technol. 36, 123003 \(2021\)](#)

Nanoscale platforms for topological superconductivity

- Engineered nanoscale systems with nontrivial topology + superconductivity
- Synthesizing topological superconductivity with Majorana zero modes

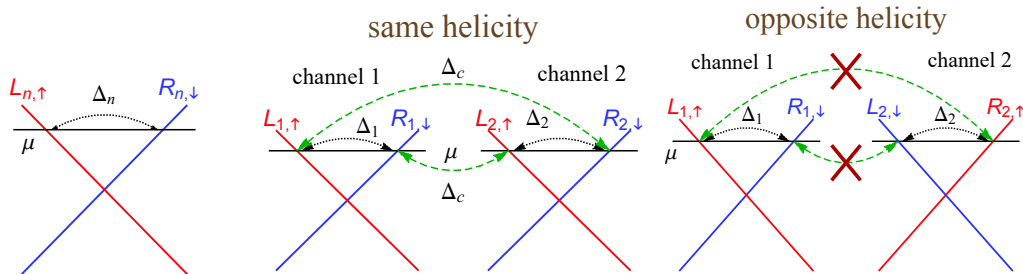


Klinovaja et al., PRB 90, 155447 (2014); [CHH et al., Phys. Rev. Lett. 121, 196801 \(2018\)](#)

- Proposals based on double helical liquids with proximity-induced pairing
⇒ time-reversal-invariant topological superconductor
 - When two parallel helical channels are in contact with a superconductor:
Cooper pairs tunnel into the channel(s), establishing the pairing of electrons in the system
⇒ proximity-induced pairing in helical channels
- * alternative platform without relying on the proximity effect: [Hung, CHH & Bansil, PRB 2025](#)

Proximity-induced pairing in helical channels

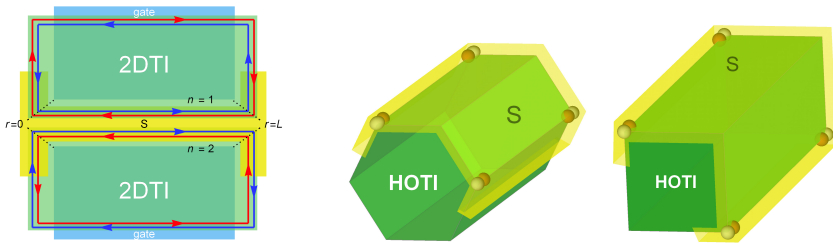
- Helical channels in contact with s -wave spin-singlet superconductor: two types of pairing processes allowed by momentum and spin conservation



- Local pairing Δ_n (channel index n): Cooper-pair partners tunnel into a single channel
- Nonlocal (crossed Andreev) pairing Δ_c : Cooper-pair partners tunnel into different channels with the same helicity

Proposals exploiting double helical liquids in 2DTI or HOTI

- Proximity effect allows nonlocal and local pairings in double helical liquids
- Local vs nonlocal pairings: competition between two gap opening mechanisms
- **Band inversion** takes place upon varying the relative strength of the local and nonlocal pairings
⇒ Majorana zero modes (MZM) emerge at system corners in the band-inverted regime
- Criterion: nonlocal pairing dominates over local pairing



Klinovaja, Yacoby and Loss, PRB 90, 155447 (2014); [CHH et al., Phys. Rev. Lett. 121, 196801 \(2018\)](#)

- Questions to be explored:
 - **tunability** of the system between topological and trivial phases?
 - **stability** of MZM against phonons in interacting systems?

Stability of the helical liquids themselves against various mechanisms

TRS preserving mechanism	R or $-\delta G$
1PB by $H_{ee,5}$ (for clean systems)	$\begin{cases} e^{-\hbar v_F k_F / (k_B T)} & \text{for } k_B T \ll \hbar v_F k_F \\ T^{2K+3} & \text{for } k_B T \gg \hbar v_F k_F \end{cases}$
1PB by $H_{ee,5}$ & $H_{imp,f}^{b,c}$	T^{2K+2}
1PB by $H_{ee,5}$ & H_{imp}^{loc}	T^{2K+2}
1PB by $H_{ee,1}$ & $H_{imp,b}^c$	T^6 for $K \approx 1$
1PB by $H_{ee,3}$ & $H_{imp,b}^{b,c}$	T^4 for $K \approx 1$
2PB by $H_{ee,3}$ & $H_{imp,f}^{c,e}$	T^{8K-2}
2PB by $H_{ee,3}$ & H_{imp}^{loc}	T^{8K-2}
Random SOI	0
Higher-order random SOI ^h (single scatterer)	For $K > 1/2$: $\begin{cases} T^{4K} & \text{for } T < T_{rso}^* \\ T^{4K} \ln^2(k_B T / \Delta_b) & \text{for } T > T_{rso}^* \end{cases}$ For $1/4 < K < 1/2$: $\begin{cases} T^{8K-2} & \text{for } T < T_{rso}^* \\ T^{4K} \ln^2(k_B T / \Delta_b) & \text{for } T > T_{rso}^* \end{cases}$
Short channel: (a single puddle)	even valley: $\begin{cases} T^4 & \text{for } k_B T \ll \delta_d \\ T^2 & \text{for } \delta_d \ll k_B T \ll E_{ch} \\ \text{const.} & \text{for } k_B T \gg E_{ch} \end{cases}$ even-odd transition: $\begin{cases} T^4 & \text{for } k_B T \ll \Gamma_t \\ \text{const.} & \text{for } \Gamma_t \ll k_B T \ll \delta_d \\ T^2 & \text{for } \delta_d \ll k_B T \ll E_{ch} \\ \text{const.} & \text{for } k_B T \gg E_{ch} \end{cases}$
1PB in charge puddles ^l (for $K \approx 1$)	odd valley: $\begin{cases} T^4 & \text{for } T \ll T_K \\ \ln^2(T/T_K) & \text{for } k_B T_K \ll k_B T \ll \delta_d \\ T^2 & \text{for } \delta_d \ll k_B T \ll E_{ch} \\ \text{const.} & \text{for } k_B T \gg E_{ch} \end{cases}$
Long channel: (averaged over puddle configurations)	$E_{ch} \ll \delta_d$: T for $k_B T \ll \delta_d$ $E_{ch} \approx \delta_d$: $1/\ln^2[\delta_d/(k_B T)]$ for $k_B T \ll \delta_d$ $E_{ch} \gg \delta_d$: $\begin{cases} 1/\ln^2[\delta_d/(k_B T)] & \text{for } k_B T \ll \delta_d' \\ 1/\ln[\delta_d/(k_B T)] & \text{for } \delta_d' \ll k_B T \ll \delta_d \end{cases}$
Noise ^l (for $K \approx 1$, long channels)	Telegraph noise: $T^2 \tanh\left(\frac{E_{ch}}{2k_B T}\right)$ 1/f noise: $\begin{cases} T^2 & \text{for } k_B T \ll E_{ch} \\ T & \text{for } k_B T \gg E_{ch} \end{cases}$
Acoustic longitudinal phonon	0

- **No influence from acoustic phonons**
to the leading order **Budich et al. PRL 2012**

Reference	Notation or name in the original work
Kainaris <i>et al</i> (2014)	$g_1 \times b$ process
Wu <i>et al</i> (2006)	H_{dis} or two-particle backscattering due to quenched disorder
Xu and Moore (2006)	Scattering by spatially random quenched impurities
Kainaris <i>et al</i> (2014)	$g_3 \times f$ process (in their class of two-particle processes)
Schmidt <i>et al</i> (2012)	$H_{V,im}^{eff}$
Kainaris <i>et al</i> (2014)	$g_3 \times b$ process (in their class of one-particle processes)
Wu <i>et al</i> (2006)	H_{hs}^l or impurity-induced two-particle correlated backscattering
Maciejko <i>et al</i> (2009)	H_2 or local impurity-induced two-particle backscattering
Lezmy <i>et al</i> (2012)	g_{2p} process or two-particle scattering
Schmidt <i>et al</i> (2012)	H_{int} or inelastic backscattering of a single electron with energy transfer to another particle-hole pair
Kainaris <i>et al</i> (2014)	g_5 process
Chou <i>et al</i> (2015)	\tilde{H}_W or one-particle spin-flip umklapp term
Kainaris <i>et al</i> (2014)	$g_5 \times f$ process (in their class of one-particle processes)
Chou <i>et al</i> (2015)	\tilde{H}_W (same notation for clean and disordered systems)
Kainaris <i>et al</i> (2014)	$g_5 \times b$ (in their class of one-particle processes)
Lezmy <i>et al</i> (2012)	g_{ie} process or inelastic scattering
Ström <i>et al</i> (2010)	H_R or randomly fluctuating Rashba spin-orbit coupling
Geissler <i>et al</i> (2014)	Random Rashba spin-orbit coupling
Kainaris <i>et al</i> (2014)	$g_{imp,b}$ process
Xie <i>et al</i> (2016)	Random Rashba backscattering
Kharitonov <i>et al</i> (2017)	\tilde{H}_R or $U(1)$ -asymmetric single-particle backscattering field
Crépin <i>et al</i> (2012)	Inelastic two-particle backscattering from a Rashba impurity

Topical review on helical liquids

[CHH et al., Semicond. Sci. Technol. 36, 123003 \(2021\)](#)

Double helical liquids

- Helical liquids formed by interacting electrons in topological edge channels $n \in \{1, 2\}$

- bosonization:

$$R_{n,\downarrow}(r) = \frac{U_{R,n}}{\sqrt{2\pi a}} e^{i[-\phi_n(r) + \theta_n(r)]}, \quad L_{n,\uparrow}(r) = \frac{U_{L,n}}{\sqrt{2\pi a}} e^{i[\phi_n(r) + \theta_n(r)]}$$

- Double helical (Tomonaga-Luttinger) liquids:

$$H_{\text{dh}} = \sum_{\delta \in \{s, a\}} \int dr \frac{\hbar u_{\delta}}{2\pi} \left[\frac{1}{K_{\delta}} (\partial_r \phi_{\delta})^2 + K_{\delta} (\partial_r \theta_{\delta})^2 \right], \quad [\phi_{\delta}(r), \theta_{\delta'}(r')] = i\delta_{\delta\delta'} \frac{\pi}{2} \text{sign}(r' - r)$$

- interaction parameters K_s, K_a :

$$K_{\delta} = \left[1 + \frac{2}{\pi \hbar v_F} (U_{ee} + \delta V_{ee}) \right]^{-1/2}$$

- $\delta \in \{s \equiv +, a \equiv -\}$: symmetric/antisymmetric combination of the two channels
- U_{ee} (V_{ee}): intrachannel (interchannel) interaction strength
- repulsive interaction: $U_{ee}, V_{ee} > 0 \Rightarrow K_s \leq K_a \leq 1$

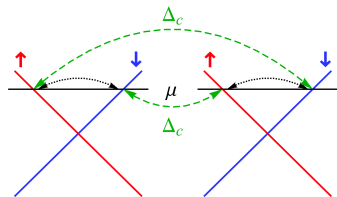
Proximity-induced pairings in double helical liquids

- Local pairing within each channel:

$$\begin{aligned}
 V_{\text{loc}} &= \int dr \frac{\Delta_1}{2} (R_1^\dagger L_1^\dagger - L_1^\dagger R_1^\dagger) + \frac{\Delta_2}{2} (R_2^\dagger L_2^\dagger - L_2^\dagger R_2^\dagger) + \text{H.c.} \\
 &= \int dr \frac{2\Delta_+}{\pi a} \cos(\sqrt{2}\theta_s) \cos(\sqrt{2}\theta_a), \quad \Delta_+ = (\Delta_1 + \Delta_2)/2
 \end{aligned}$$

- Nonlocal pairing between different channels:

$$\begin{aligned}
 V_{\text{cap}} &= \int dr \frac{\Delta_c(r)}{2} \left[(R_1^\dagger L_2^\dagger - L_2^\dagger R_1^\dagger) + (R_2^\dagger L_1^\dagger - L_1^\dagger R_2^\dagger) \right] + \text{H.c.} \\
 &= \int_0^L dr \frac{2\Delta_c}{\pi a} \cos(\sqrt{2}\theta_s) \cos(\sqrt{2}\phi_a)
 \end{aligned}$$



- Criterion for band inversion and topological zero modes:

$$\Delta_c^2 + \Delta_-^2 > \Delta_+^2 \quad \Rightarrow \quad |\Delta_c| > |\Delta_+| \quad (\text{for } \Delta_1 = \Delta_2 = \Delta_+)$$

\Rightarrow nonlocal pairing dominates over local pairing

Electron-phonon-coupled system

- Phonon-induced terms in the Hamiltonian: $H_{\text{ph}} + H_{\text{ep}}$
- Phonon subsystem:

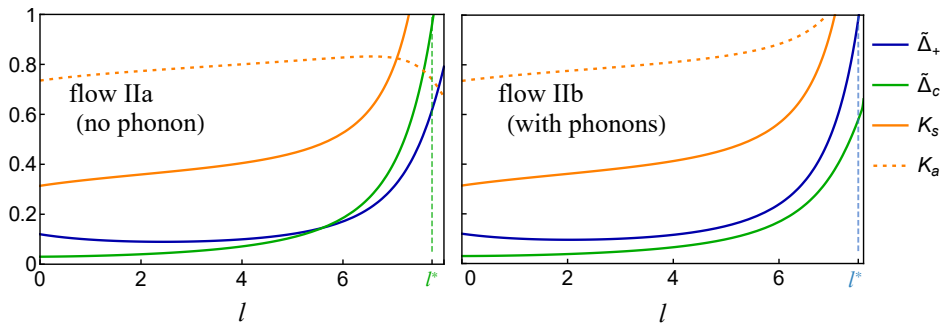
$$H_{\text{ph}} = \sum_n \int \frac{dr}{2\rho} \left[\pi_n^2 + \rho^2 c^2 (\partial_r d_n)^2 \right]$$

- c : phonon velocity
- ρ : mass density of lattice
- d_n : displacement field due to phonons
- π_n : conjugate field of d_n
- Electron-phonon coupling (strength g): deformation potential coupled to charge density

$$H_{\text{ep}} = \sum_n g \int dr (\partial_r \phi_n) (\partial_r d_n)$$

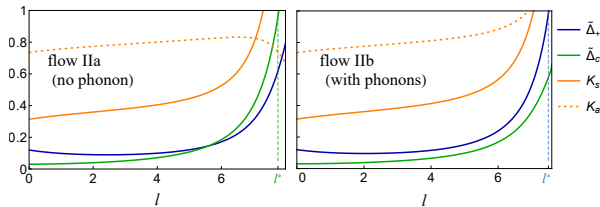
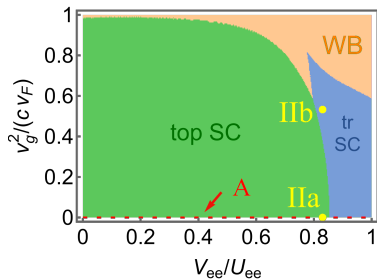
- Perturbative analysis:
acoustic phonons have no leading-order effects on helical liquids
[Budich et al., PRL 2012](#)
- We treat $H_{\text{dh}} + H_{\text{ph}} + H_{\text{ep}}$ **non-perturbatively**: renormalization-group (RG) analysis

RG flow without phonons vs RG flow with phonons



- Renormalized pairing strengths: local Δ_+ versus nonlocal Δ_c
- Direct comparison of the RG flows: observing how phonons modify the flows
- Distinct behaviors in the RG flows of K_a : flowing to larger values with phonons \Rightarrow favoring local over nonlocal pairing
- **Opposite outcomes** for topological properties despite identical initial parameters

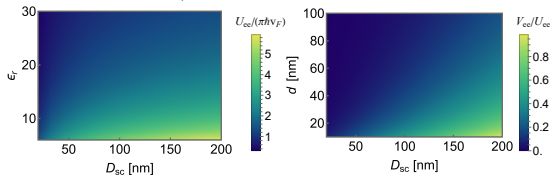
e - e interaction and phonon effects on topological phase diagram



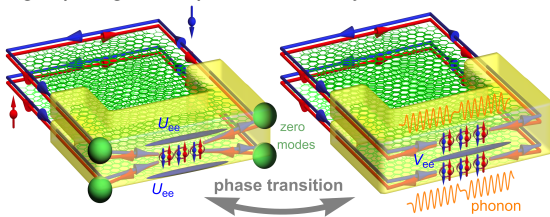
- e-ph coupling: $g \propto v_g^2/(cv_F)$ • interchannel (V_{ee}) and intrachannel (U_{ee}) interaction strengths
- Phonons: effectively mediate attractive interactions within each channel
 \Rightarrow enhancing local pairing Δ_n more significantly (compared to Δ_c)
- Electron-phonon coupling can push the system from topological SC to trivial SC phase
 \Rightarrow **phonon-induced topological phase transitions**

Tunable platform for topological superconductivity

- Electrically tunable topological phase transitions
 - Intrachannel U_{ee} : screening length D_{sc} and dielectric constant ϵ_r of insulating layers
 - Interchannel-to-intrachannel ratio V_{ee}/U_{ee} : D_{sc} , ϵ_r and interlayer separation d

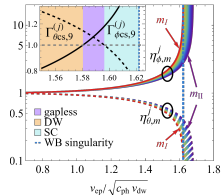
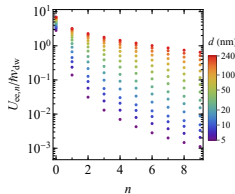
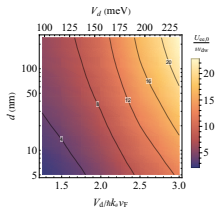
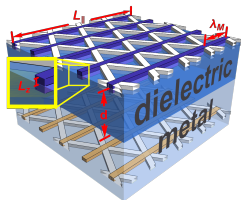


- Omnipresence of $e-e$ interactions and phonons
 \Rightarrow constraints in realizing topological superconductivity and zero modes



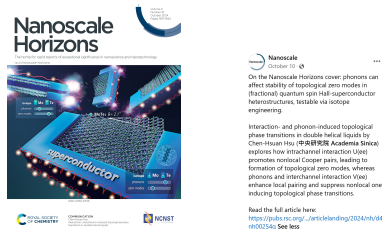
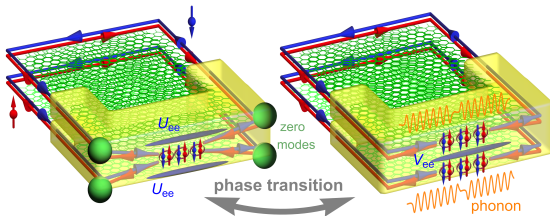
Summary

- Electrically tunable domain wall network as a platform for strongly correlated systems



Wang and CHH, 2D Mater. 11, 035007 (2024)

- Electrically tunable phase transitions between topological and trivial superconductivity



CHH, Nanoscale Horiz. 9, 1725 (2024); highlighted on the journal cover

Additional works and open positions

- Fractional excitations, (fractional) quantum anomalous Hall effect, gapless chiral edge modes from moiré umklapp scatterings in TBG
[CHH et al., Phys. Rev. B 108, L121409 \(2023\)](#)
- Spin helix in domain wall network of twisted bilayer graphene
[Y.-Y. Chang, K. Saito, and CHH, arXiv:2412.14065 \(under review\)](#)
- Quasiperiodicity-induced localization in non-Hermitian systems
[Y.-P. Wang, C.-K. Chang, R. Okugawa, and CHH \(under review\)](#)
- Time-reversal soliton pairs in high spin Chern insulators
[Y.-C. Hung, B. Wang, CHH, A. Bansil, and H. Lin, Phys. Rev. B 110, 035125 \(2024\)](#)
- Magnetic field-free platforms for topological superconductivity
[Y.-C. Hung, CHH, and A. Bansil, Phys. Rev. B 111, 245145 \(2025\)](#)

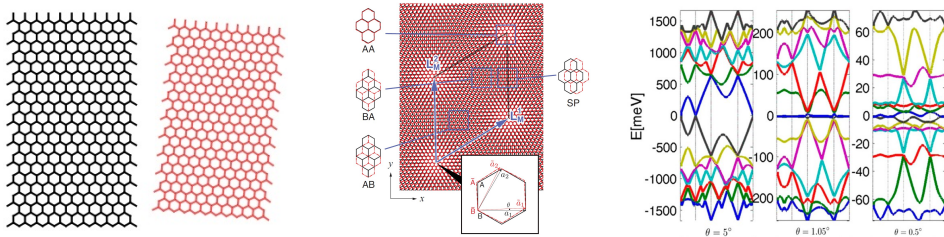
- Open positions in Quantum Matter Theory
 - <https://sites.google.com/view/qmtheory>
 - Welcome highly motivated postdocs, assistants and students!
 - Follow us on X: [hbar_FanClub](#)



Technical details

Moiré bilayer systems in 2D twisted nanostructures

- Twist angle between two graphene monolayers:
a tunable parameter allowing for continuously varying the band structure



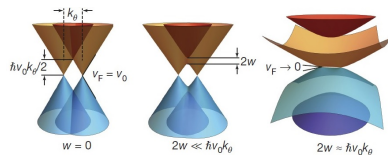
Nam and Koshino, PRB 2017 Bistritzer and MacDonald, PNAS 2011

- (Quasi-)flat bands close to the magic angle ($e-e$ interaction $>$ bandwidth \approx kinetic energy)
 \Rightarrow a platform for strongly correlated electron systems
- Observations on superconductivity and correlated insulators (Jarillo-Herrero group)
Cao et al., Nature 556, 43 (2018); Cao et al., Nature 556, 80 (2018), and many more!
- Early studies on lattice mismatch-induced moiré structures in MoS₂/WSe₂ heterobilayers
Shih group: Zhang et al., Sci. Adv. 3, e1601459 (2017)

Continuum model for TBG

- Single-particle Hamiltonian: hybridization of Dirac cones in the two layers

$$H_{\text{sp}} = \begin{pmatrix} H_{\gamma\sigma}^{(t)} & T_{\gamma}(\mathbf{x}) \\ T_{\gamma}^{\dagger}(\mathbf{x}) & H_{\gamma\sigma}^{(b)} \end{pmatrix}$$



Cao et al., Nature 2018

- basis: $(c_{A\gamma\sigma}^t, c_{B\gamma\sigma}^t, c_{A\gamma\sigma}^b, c_{B\gamma\sigma}^b)^T$
- Dirac Hamiltonian for the TBG with a twist angle θ :

$$H_{\gamma\sigma}^{(\eta)} = \begin{pmatrix} -\eta V_d & \gamma \hbar v_F |\mathbf{k}| e^{-i\gamma(\theta_k - \eta\theta/2)} \\ \gamma \hbar v_F |\mathbf{k}| e^{i\gamma(\theta_k - \eta\theta/2)} & -\eta V_d \end{pmatrix}$$

- θ_k : angle of the momentum direction; V_d : interlayer bias; η : layer index; γ : valley index
- Interlayer hybridization (with the 2D coordinate \mathbf{x}):

$$T_{\gamma}(\mathbf{x}) = \frac{w}{3} \sum_{j=1}^3 e^{i\gamma \mathbf{q}_j \cdot (\mathbf{x} + \mathbf{x}_0)} T_{\gamma,j}, \quad T_{\gamma,1} = \begin{pmatrix} 1 & 1 \\ 1 & 1 \end{pmatrix}, \quad T_{\gamma,2} = (T_{\gamma,3})^* = \begin{pmatrix} e^{i2\gamma\pi/3} & 1 \\ e^{-i2\gamma\pi/3} & e^{i2\gamma\pi/3} \end{pmatrix}$$

- $\mathbf{q}_1 \equiv -k_{\theta} \mathbf{e}_y$, $\mathbf{q}_2 \equiv k_{\theta} (\frac{\sqrt{3}}{2} \mathbf{e}_x + \frac{1}{2} \mathbf{e}_y)$, $\mathbf{q}_3 \equiv k_{\theta} (-\frac{\sqrt{3}}{2} \mathbf{e}_x + \frac{1}{2} \mathbf{e}_y)$, and $k_{\theta} \equiv \frac{8\pi}{3a_0} \sin(\theta/2)$

Bistritzer and MacDonald, PNAS 2011; Efimkin and MacDonald, PRB 2018

Low-energy effective model

- For sufficiently large V_d , the continuum model H_{sp} can be projected onto the conduction band of the top layer and the valence band of the bottom layer
- Low-energy effective model: describing massive Dirac fermion

$$\begin{pmatrix} \hbar v_F |\mathbf{k}| & -\gamma \Delta_- \cos \theta_k - i \Delta_+ \sin \theta_k \\ -\gamma \Delta_- \cos \theta_k + i \Delta_+ \sin \theta_k & -\hbar v_F |\mathbf{k}| \end{pmatrix}$$

- effective mass from the interlayer hybridization:

$$\Delta_{\pm, \gamma} \equiv \frac{|T_{\gamma}^{AB}| \pm |T_{\gamma}^{BA}|}{2}$$
$$\phi_{\pm, \gamma} \equiv \frac{\arg(T_{\gamma}^{AB}) \pm \arg(T_{\gamma}^{BA})}{2}$$

- spatial dependence in Δ_- : a spatially dependent sign of mass (i.e., spectral gap)
- mapped to a $(p_x \pm ip_y)$ **superconductor**:
 \Rightarrow gapless modes between domains with opposite mass set by $\text{sign}(\gamma \Delta_-)$

Helical Tomonaga-Luttinger liquids

- Bosonization:

$$R_{\downarrow}(r) = \frac{U_R}{\sqrt{2\pi a}} e^{i[-\phi(r)+\theta(r)]}, \quad L_{\uparrow}(r) = \frac{U_L}{\sqrt{2\pi a}} e^{i[\phi(r)+\theta(r)]}$$

- *Helical Tomonaga-Luttinger liquid:*

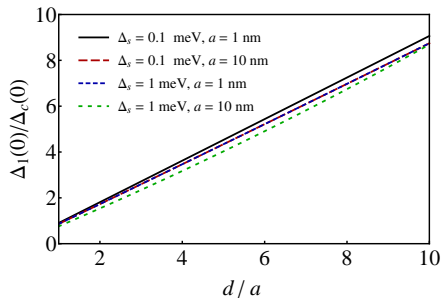
$$H = \frac{\hbar u}{2\pi} \int dr \left[\frac{1}{K} (\partial_r \phi)^2 + K (\partial_r \theta)^2 \right], \quad [\phi(r), \theta(r')] = i \frac{\pi}{2} \text{sign}(r' - r)$$

- $K = 1$ for noninteracting systems; $K < 1$ for repulsive interaction
- Local density of states: universal scaling behavior

$$\rho_{\text{dos}}(E, T) \propto T^{\alpha} \cosh \left(\frac{E}{2k_B T} \right) \left| \Gamma \left(\frac{1 + \alpha}{2} + i \frac{E}{2\pi k_B T} \right) \right|^2$$

- Interaction parameter K can be extracted through $\alpha = (K + 1/K)/2 - 1$

Estimated bare gap ratio



estimated from source-term approach:

$$\frac{\Delta_1(0)}{\Delta_c(0)} \approx \frac{d}{a} \frac{e^{d/\xi_s} K_0\left(\frac{\Delta_s a}{\hbar v_F}\right)}{K_0\left(\frac{\Delta_s a}{2\hbar v_F}\right) I_0\left(\frac{\Delta_s a}{2\hbar v_F}\right)}$$

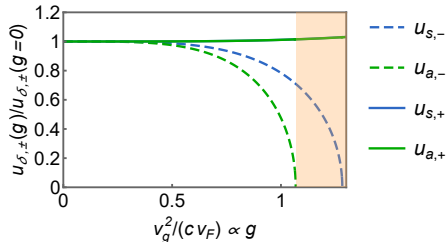
- d : inter-hinge separation, v_F : Fermi velocity, a : hinge state width, I_0 , K_0 : modified Bessel functions, Δ_s , ξ_s : pairing gap and coherence length of the parent superconductor
- $\frac{\Delta_1(0)}{\Delta_c(0)}$ depends weakly on Δ_s and a (except for linear dependence on d/a)
- For $\Delta_s \in [0.1 \text{ meV}, 1 \text{ meV}]$ and $a \in [1 \text{ nm}, 10 \text{ nm}]$, $\Delta_1(0)/\Delta_c(0) \sim O(1) - O(10)$

Influence of electron-phonon coupling: excitation velocities

- $H_{\text{dh}} + H_{\text{ph}} + H_{\text{ep}}$: incorporating both e - e interactions and phonons in a **non-perturbative** way
- Hybridization of electron and phonon modes leads to modifications of excitation velocity:

$$u_{\delta,\eta} = \sqrt{\frac{u_{\delta}^2 + c^2}{2} + \frac{\eta}{2} \sqrt{(u_{\delta}^2 - c^2)^2 + 4v_g^4}}, \quad \text{with} \quad \begin{cases} \delta \in \{s, a\}, \\ \eta \in \{+, -\}, \end{cases} \quad \text{and} \quad v_g \propto g^{1/2}$$

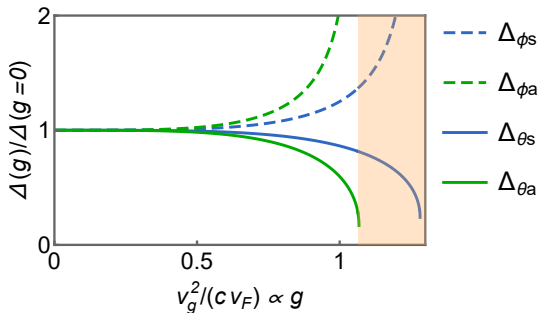
⇒ quantifying how electron-phonon coupling alters excitation dynamics



- Phonon-induced modified velocity vanishes
⇒ Wentzel-Bardeen singularity in 1D systems [Wentzel 1951](#); [Bardeen 1951](#); [Loss & Martin PRB 1994](#)

Influence of electron-phonon coupling: scaling dimensions

- Electron-phonon coupling $g \propto v_g^2$ influences the scaling dimensions of various operators



- Larger g values decrease the scaling dimensions of $e^{i\theta_s}$, $e^{i\theta_a}$, while increasing those of $e^{i\phi_s}$, $e^{i\phi_a}$
 - \Rightarrow enhancing pairing instability and suppressing density wave instability
 - \Rightarrow equivalent to **attractive interactions**
- Electron-phonon coupling alters the scaling dimensions of pairing operators
 - \Rightarrow expecting effects on phase diagram through scaling dimensions

Pairing strengths renormalized by e - e interactions

- Renormalization-group (RG) flow equations with the cutoff $a(l) = a(0)e^l$:

$$\frac{d\tilde{\Delta}_+}{dl} = \left[2 - \frac{1}{2} \left(\frac{1}{K_s} + \frac{1}{K_a} \right) \right] \tilde{\Delta}_+$$

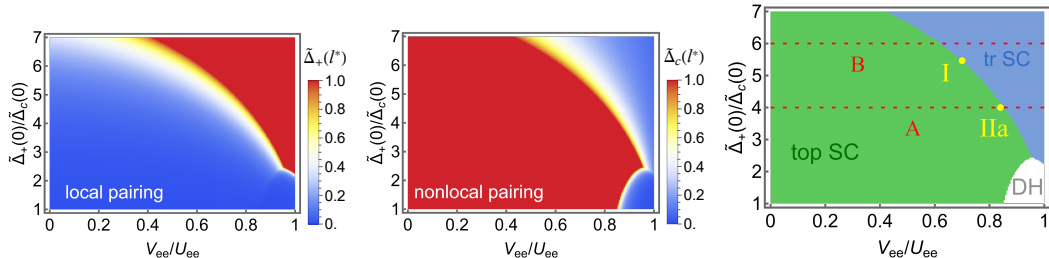
$$\frac{d\tilde{\Delta}_c}{dl} = \left[2 - \frac{1}{2} \left(\frac{1}{K_s} + K_a \right) \right] \tilde{\Delta}_c$$

$$\frac{dK_s}{dl} = 2\tilde{\Delta}_+^2 + 2\tilde{\Delta}_c^2$$

$$\frac{dK_a}{dl} = 2\tilde{\Delta}_+^2 - 2K_a^2\tilde{\Delta}_c^2$$

- dimensionless couplings: $\tilde{\Delta}_+ = \Delta_+/\Delta_a$, $\tilde{\Delta}_c = \Delta_c/\Delta_a$ • Δ_a : bandwidth
- For each set of initial parameters at $l = 0$, we numerically solve the RG flow equations
 - to extract the renormalized local and nonlocal pairings at the end of the RG flow $l = l^*$
 - to examine the topological criterion through the relative strengths $\Delta_+(l^*)$ vs $\Delta_c(l^*)$

Interaction effects on the phase diagram in the absence of phonons



- RG analysis to examine $e-e$ interaction effects on local Δ_+ and nonlocal Δ_c pairings
- Various phases: topological/trivial SC (top/tr SC) & double helical liquid (DH)
- Intrachannel interaction U_{ee} suppresses Δ_+ more than Δ_c
- Interchannel interaction V_{ee} reduces Δ_c :
sufficiently large V_{ee} induces phase transition towards trivial superconductivity
 \Rightarrow suppressing topological zero modes
- **Tunability** provided by controlling the ratios of V_{ee}/U_{ee} and $\Delta_+(0)/\Delta_c(0)$

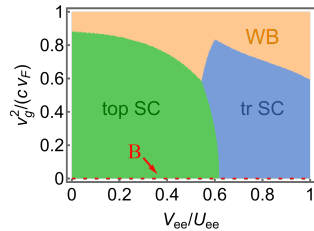
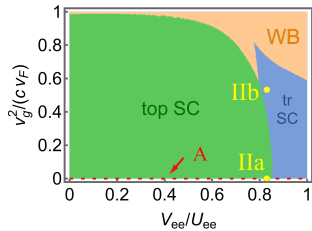
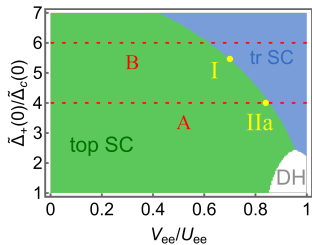
RG flow analysis including e - e interaction and phonon influences

- RG flow equations with the cutoff $a(l) = a(0)e^l$ and channel index $n \in \{1, 2\}$:

$$\begin{aligned}\frac{d\tilde{\Delta}_+}{dl} &= \left[2 - \frac{1}{2} \sum_{\eta=\pm} \left(\frac{u_s \gamma_{s,\eta}^\theta}{K_s u_{s,\eta}} + \frac{u_a \gamma_{a,\eta}^\theta}{K_a u_{a,\eta}} \right) \right] \tilde{\Delta}_+ \\ \frac{d\tilde{\Delta}_c}{dl} &= \left[2 - \frac{1}{2} \sum_{\eta=\pm} \left(\frac{u_s \gamma_{s,\eta}^\theta}{K_s u_{s,\eta}} + \frac{K_a u_a \gamma_{a,\eta}^\phi}{u_{a,\eta}} \right) \right] \tilde{\Delta}_c \\ \frac{dK_s}{dl} &= 2\tilde{\Delta}_+^2 + 2\tilde{\Delta}_c^2 \\ \frac{dK_a}{dl} &= 2\tilde{\Delta}_+^2 - 2K_a^2 \tilde{\Delta}_c^2\end{aligned}$$

- Δ_a : bandwidth
- dimensionless couplings: $\tilde{\Delta}_+ = \Delta_+/\Delta_a$, $\tilde{\Delta}_c = \Delta_c/\Delta_a$
- dimensionless parameters $\gamma_{\delta,\eta}^\phi$, $\gamma_{\delta,\eta}^\theta$ (depending on the modified excitation velocities)
- For each set of initial parameters at $l = 0$, we numerically solve the RG flow equations
 - to extract the renormalized local and nonlocal pairings at the end of the RG flow $l = l^*$
 - to examine the topological criterion through the relative strengths $\Delta_+(l^*)$ vs $\Delta_c(l^*)$

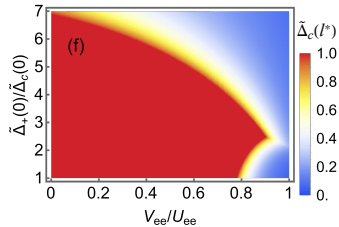
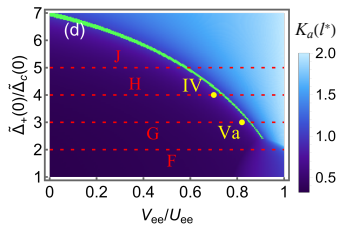
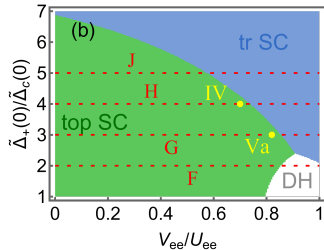
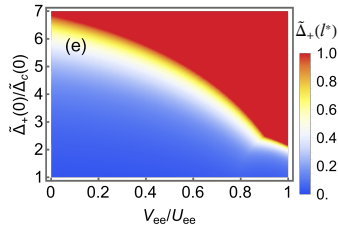
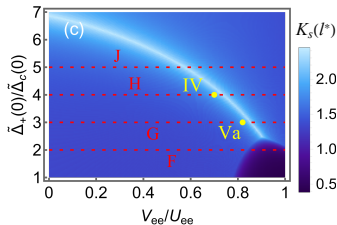
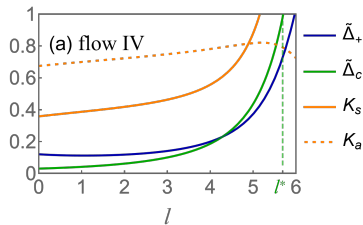
More numerical analysis - I



- Phase diagrams for different initial values of the local-to-nonlocal gap ratio $\tilde{\Delta}_n(0)/\tilde{\Delta}_c(0)$

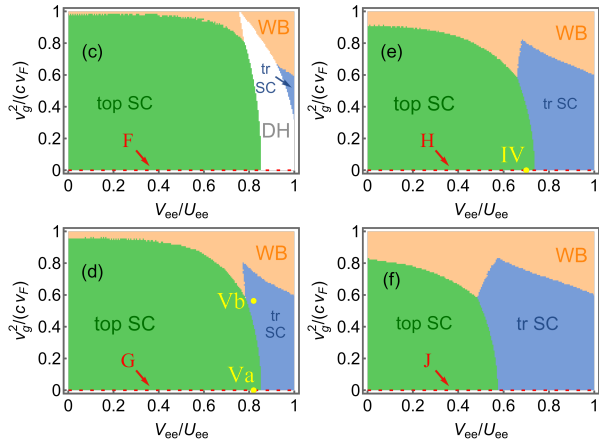
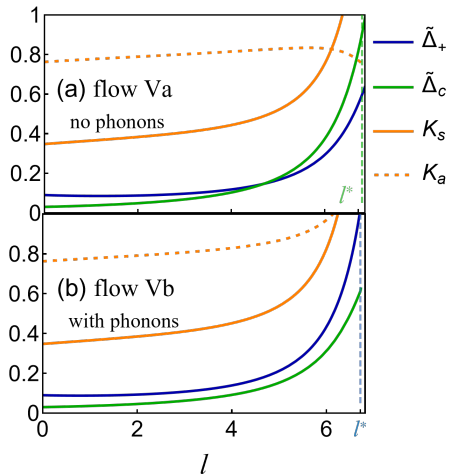
More numerical analysis - II

- Phase diagram without phonons for $U_{ee}/(\pi\hbar v_F) = 2$ and $\tilde{\Delta}_c(0) = 0.03$

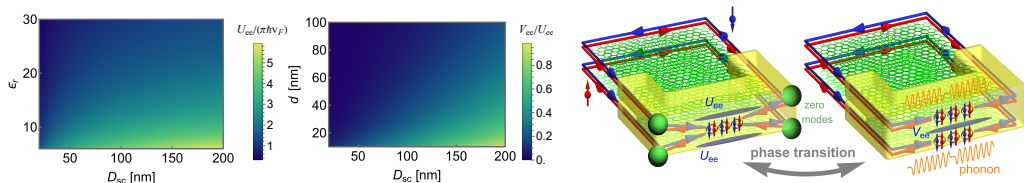


More numerical analysis - III

- RG flow and phase diagrams for $U_{ee}/(\pi\hbar v_F) = 2$ and $\tilde{\Delta}_c(0) = 0.03$



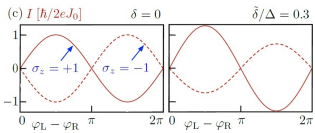
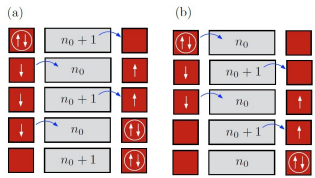
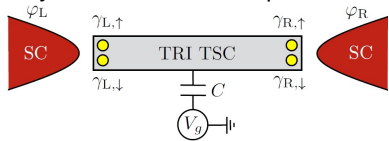
Electrically tunable topological phase transition



- Intrachannel interaction U_{ee} :
tunable by screening length D_{sc} and dielectric constant ϵ_r of insulating layers
- Interchannel-to-intrachannel interaction strength ratio V_{ee}/U_{ee} :
tunable by D_{sc} , ϵ_r and interlayer separation d
- One can induce phase transitions by varying the strengths of U_{ee} and V_{ee}
 \Rightarrow monitoring the presence/absence of topological zero modes
- Our results indicate electrically tunable topological phase transitions in double helical liquids

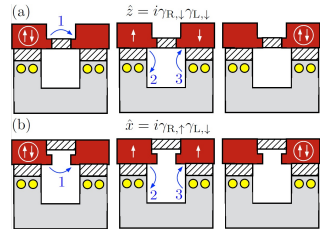
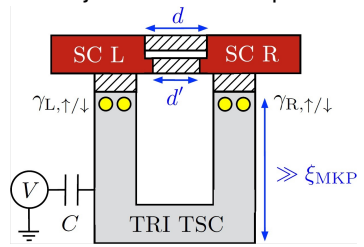
Proposals for MKP detection and quantum computing

Parity-controlled 2π Josephson effect



Schrade and Fu, PRL 120, 267002 (2018)

Majorana Kramers qubit



Schrade and Fu, PRL 129, 227002 (2022)